



Temporal relationship of the orphan receptor TR3 translocation and expression with zinc-induced apoptosis in prostate cancer cells

Ding Ma, Yuchen Guo, Yongqiang Fu, Jinfeng Wu, Ruimin Ren

Department of Urology, Shanxi Bethune Hospital, Shanxi Academy of Medical Sciences, Tongji Shanxi Hospital, Third Hospital of Shanxi Medical University, Taiyuan, China

Contributions: (I) Conception and design: D Ma; (II) Administrative support: R Ren, J Wu; (III) Provision of study materials or patients: D Ma; (IV) Collection and assembly of data: Y Guo, Y Fu; (V) Data analysis and interpretation: R Ren; (VI) Manuscript writing: All authors; (VII) Final approval of manuscript: All authors.

Correspondence to: Ruimin Ren. Department of Urology, Shanxi Bethune Hospital, Shanxi Academy of Medical Sciences, Tongji Shanxi Hospital, Third Hospital of Shanxi Medical University, Taiyuan 030032, China. Email: 408843057@qq.com.

Background: This study aimed to investigate the precise mechanism of zinc-induced apoptosis in human prostate cell lines PC-3 and LNCaP and explore its relationships with the translocation and expression of the orphan receptor TR3 and cytochrome c.

Methods: The effects of zinc exposure on apoptosis levels were examined in both PC-3 and LNCaP cells. These cells were treated with exogenous ZnCl₂ (100 μM) for 0, 4, 8, 12, and 24 h. Dansylaminoethyl-cyclen (DAEC) fluorescent probe was applied to visualize cellular zinc localization. Zinc-induced apoptosis was identified by Hoechst nuclear staining and flow cytometry analysis. TR3 messenger RNA (mRNA) expression levels were detected by real time-quantitative polymerase chain reaction (PCR). TR3 protein localization and mitochondrial release of cytochrome c were identified by immunofluorescence microscopy. Mitochondrial membrane potential collapse under fluorescence microscopy was examined with a MitoLight probe.

Results: Zinc exposure led to gradually increasing apoptosis levels in both LNCaP and PC-3 cells over the 24-h treatment period. The apoptotic effects could be observed as early as after 4 h of zinc treatment in PC-3 cells, with this being seen at 8 h in LNCaP cells. The apoptosis levels of both PC-3 and LNCaP cells began to increase significantly from 8 to 24 h when necrotic cells were also found. TR3 protein translocation from the nucleus to the mitochondria was noted and was accompanied by cytochrome c release into the cytosol from the mitochondria. Interestingly, no significant changes in TR3 mRNA expression levels were observed after zinc treatment. However, the mitochondrial membrane potential of both PC-3 and LNCaP cells gradually disappeared following extended zinc exposure.

Conclusions: Zinc-induced apoptosis could be regulated through TR3 protein translocation from the nucleus to the mitochondria in prostate cancer cells without notable changes in TR3 mRNA levels. The direct effect of zinc on the mitochondria was associated with the release of cytochrome c into the cytosol through the mitochondrial targeting of TR3 protein.

Keywords: Zinc; apoptosis; prostate cancer; the orphan receptor TR3; cytochrome c

Submitted Dec 26, 2022. Accepted for publication Mar 21, 2023. Published online Mar 28, 2023.

doi: 10.21037/tau-23-61

View this article at: <https://dx.doi.org/10.21037/tau-23-61>

Introduction

Background

Prostate cancer has the second highest incidence rate among cancers in males worldwide, being only behind lung cancer (1). Although androgen deprivation therapy and radical prostatectomy can significantly improve the prognosis of patients with prostate cancer, some still have ineffective clinical outcomes, leading to disease progression (2). Recent reports have suggested that complex molecular mechanisms contribute to prostate cancer, including factors such as hormones, neuroendocrine differentiation, epithelial-mesenchymal transition, genetic susceptibility, environmental factors, and others (3-5). A better understanding of these mechanisms will lead to better preventative strategies, enhanced diagnosis, and improved management.

Rationale and knowledge gap

Zinc has been shown to be present at higher concentrations in the peripheral zone of healthy prostate tissue. However, when prostate epithelial cells undergo malignant transformation in

the peripheral zone, the zinc levels are strikingly decreased and inversely correlated with disease progression (6). The mechanisms by which zinc can affect apoptosis and metabolism of prostate cells include the increase in the BCL2-Associated X (Bax) to B-cell lymphoma-2 (Bcl-2) ratio, which induces hypoxia-inducible factor-1 α (HIF-1 α) degradation, leading to decreased expression of apoptosis inhibitor protein Survivin. In addition, zinc has been shown to suppress the metastatic potential of prostate cancer by inhibiting nuclear factor κ B (NF- κ B) signaling (7).

Objective

A variety of organic or inorganic substances could increase the level of apoptosis in prostate cancer, previous study indicated that taurine promoted apoptosis and inhibited proliferation of prostate cancer cells in a dose-dependent manner (8). Zinc can change the permeability of mitochondrial membrane, leading to the release of related substances in mitochondria into the cytoplasm, thus mediating the apoptosis in prostate cancer cells (9); zinc-mediated mitochondrial apoptosis plays an important role in the treatment of prostate cancer; however, few studies have sought to clarify the specific mechanisms involved and treatment methods. In this study, both PC-3 (hormone refractory prostate cancer cell) and LNCaP (hormone sensitive prostate cancer cell) cells were incubated with zinc for variable durations, and apoptosis levels were detected. Furthermore, we explored the possible mechanism of zinc-induced apoptosis related to the translocation and expression of orphan receptor TR3 and cytochrome c in both PC-3 and LNCaP cells. We present the following article in accordance with the MDAR reporting checklist (available at <https://tau.amegroups.com/article/view/10.21037/tau-23-61/rc>).

Methods

Cell culture

The human prostate cancer cell lines PC-3 and LNCaP (obtained from Cell Resource Center of the Institute of Life Sciences, Shanghai, China) were cultured in RPMI 1640 medium with glutamine plus 10% fetal bovine serum (FBS) (BC-SE-FBS01C; Nanjing Biochannel Biotechnology Co., Ltd., Nanjing, China) and 1% penicillin/streptomycin. Cells were maintained at 37 °C in a humidified atmosphere with 5% CO₂.

Highlight box

Key findings

- Zinc could lead to gradually increasing apoptosis levels in both LNCaP and PC-3 cells, the mechanism mediated by the translocation of TR3 and cytochrome c.

What is known and what is new?

- Zinc has been shown to be present at higher concentrations in the peripheral zone of healthy prostate tissue. The zinc levels are strikingly decreased and inversely correlated with disease progression of prostate cancer. The mechanism of zinc-mediated mitochondrial apoptosis in prostate cancer has not been exhaustively investigated;
- Zinc-induced apoptosis could be regulated through TR3 protein translocation from the nucleus to the mitochondria in prostate cancer cells without notable changes in TR3 mRNA levels, TR3 protein targeted the release of cytochrome c into the cytosol and lead to the apoptosis of prostate cancer cells. Zinc can play an inhibitory role in prostate cancer by inducing apoptosis, and TR3 is expected to be a new target for the development of novel treatment methods for this disease.

What is the implication, and what should change now?

- Our study implicated the potential use of zinc as an antitumor agent to treat prostate cancer.

Cell growth and treatment with zinc

Both PC-3 and LNCaP cell lines were subcultured until they reached 70% confluency; they were then washed twice with phosphate-buffered saline (PBS) (ZLI-9062; Zhongshan Golden Bridge Biotechnology Co., Ltd., Beijing, China) and dissociated with 0.25% Trypsin (ZLI-9010; Zhongshan Golden Bridge Biotechnology Co. Ltd.). Before being treated with zinc (ZnCl₂; 012307; Sigma-Aldrich, St. Louis, MO, USA), both cell lines were seeded in 24-well plates (FCP243; Beyotime Biotechnology Co., Ltd., Shanghai, China) at a density of 1×10⁵ cells per well and allowed to attach overnight. Cells were subsequently treated with zinc (100 μM) for 0, 4, 8, 12, or 24 h.

Distribution of zinc in prostate cancer cells

Before being harvested, the PC-3 and LNCaP cells were washed twice with PBS to remove extracellular zinc. To visualize intracellular dansylaminoethyl-cyclen (DAEC)-sensitive Zn²⁺, DAEC (10 μM; Dojin Chemical Laboratories, Tokyo, Japan) was added and incubated for 10 min at 37 °C. Cells were then washed with PBS, centrifuged (1,000 r/min for 5 min), resuspended in 100 μL PBS, and then observed under fluorescence microscopy (Olympus Corporation, Tokyo, Japan).

Measurement of intracellular zinc uptake

Methods using DAEC followed the manufacturer's protocol. Briefly, after being treated with zinc, DAEC (10 μM) was added and incubated for 10 min at 37 °C. Cells were washed with PBS, centrifuged, and resuspended in PBS at 1×10⁶ cells/mL in cuvettes. The fluorescence intensity of each cell suspension was measured at room temperature with a fluorescence spectrophotometer (F4700, Hitachi, Tokyo, Japan) at excitation and emission wavelengths of 323 and 528 nm, respectively (slit widths 5 nm). The zinc levels in cells were estimated using a standard curve, which was generated by adding increasing amounts of ZnCl₂ into a solution of 10 μM DAEC in PBS.

Apoptosis analysis

Both PC-3 and LNCaP cells were cultured as described above. After exposure to exogenous zinc for different durations, Hoechst 33342 (B2261; Sigma-Aldrich) was added to the cell lines. Changes in nuclear morphology

were observed under a fluorescence microscope using a filter for Hoechst 33342 (365 nm). For staining quantification, the percentages of Hoechst-positive nuclei per optical field were counted. Additionally, apoptosis levels were determined with a fluorescein-isothiocyanate-labeled annexin/propidium iodide (PI) apoptosis detection kit (A211-01; Vazyme Biotech Co., Ltd., Nanjing, China) following the manufacturer's protocol. After zinc treatment, floating cells and trypsinized cells were collected and washed twice with a mixture of binding buffer, 10 mM of HEPES/sodium hydroxide (pH 7.4), 140 mM of NaCl and 2.5 mM of calcium chloride. The cells were dissolved in buffer at 1×10⁵ cells/mL and subsequently incubated with Annexin-fluorescein isothiocyanate (FITC)/PI in the dark for 15 min at room temperature. The samples were analyzed within 1 h with a FACScan instrument (No. 349202; BD Biosciences, Franklin Lakes, NJ, USA).

Quantitative real-time polymerase chain reaction (qRT-PCR) analysis

Total cellular RNA was extracted from PC-3 and LNCaP cells with the Rneasy Mini Kit (74104; Qiagen, Hilden, Germany) according to the manufacturer's protocols. Briefly, 2 μg of total RNA was extracted and converted into first strand complement DNA (cDNA) using the Superscript II reverse transcriptase and random primers (18091050; Invitrogen, Thermo Fisher Scientific, Waltham, MA, USA). qRT-PCR analysis was performed on an ABI Prism 7300 Sequence Detection System (SDS) using the SYBR Green PCR Master Mix (Applied Biosystems, Thermo Fisher Scientific). The 20 μL of PCR (in triplicate) consisted of 10 μL of SYBR Green PCR Master Mix, 1 μL of 5 μM forward and reverse primers, 8 μL of nuclease-free water, and 1 μL of template cDNA. Cycling was performed using the default conditions of the ABI 7300 SDS software (v. 1.3.1). Relative gene expression values were normalized to that of 18S ribosomal RNA (rRNA). The primers were as follows: TR3 (5'-CCGAACCGTGACACTTCC-3'; 5'-CTTGCAGCCCTCACAGGT-3') and 18S rRNA (5'-AATTTGACTCAACACGGGAAACCTCAC-3'; 5'-CAACAAATCGCTCCACCAACTAAGAAC-3'). The thermal cycling program was 3 min at 95 °C for enzyme activation (allowing an automated hot start PCR), followed by 45 cycles of denaturation for 30 s at 95 °C, 30 s of annealing at 60 °C, and 30 s of extension at 72 °C. As a negative control for the primers, a no-template cDNA PCR reaction was run under the same conditions.

Immunofluorescence staining

Both PC-3 and LNCaP cells were cultured and treated with zinc as required, and immunofluorescence staining was performed. Briefly, after being washed with PBS, the cells were fixed with 4% paraformaldehyde for 15 min at room temperature. To identify TR3 protein expression, cells were first incubated with an anti-TR3 immunoglobulin G (IgG) antibody (sc365113; Santa Cruz Biotechnology Inc., Dallas, TX, USA) and then with a corresponding FITC-conjugated anti-IgG antibody (AS10115; Agrisera, Vasterbotten, Sweden) as the secondary antibody. To visualize nuclei, cells were stained with 50 µg/mL of 4,6-diamidino-2-phenylindole (B28718; Sigma-Aldrich) containing 100 mg/mL of Dnase-free Rnase A. To visualize mitochondria, cells were incubated with an anti-HSP60 mouse IgG antibody (sc136291; Santa Cruz Biotechnology, Inc.) and reacted with a Texas red-conjugated anti-mouse IgG (sc69786; Santa Cruz Biotechnology, Inc.) as the secondary antibody.

Additionally, to display the translocation of cytochrome c in PC-3 and LNCaP cells, the experimental procedure was performed as described by the manufacturer's protocol. Cells were incubated with an anti-cytochrome c antibody (sc13156; Santa Cruz Biotechnology, Inc.) and then the FITC-conjugated antibody. Immunofluorescence staining procedures for both nuclei and mitochondria were then conducted.

Visualization of mitochondrial permeability transition

Mitochondrial membrane potential changes were assayed with MitoLight dye according to manufacturer's instructions (C1048; Millipore, Burlington, MA, USA). After treatment with zinc, cells were incubated with prediluted MitoLight solution for 30 min. Cells were washed twice with 1× incubation buffer, mounted with coverslips, and observed immediately under a fluorescence microscope.

Statistical analysis

Statistical analyses were performed using SPSS 20.0 software (IBM Corp., Armonk, NY, USA). Data for continuous variables are expressed as the mean ± standard deviation. Statistical analysis was performed independently using the Student's *t*-test, and significance was defined as $P < 0.05$. All the experiments were replicated three times.

Results

Zinc accumulation and intracellular zinc density in PC-3 and LNCaP cell lines

First, we investigated the zinc distribution in both PC-3 and LNCaP cells treated with zinc by using a zinc-sensitive fluorescent probe (DAEC) observed under a fluorescence microscope. As shown in *Figure 1A*, little DAEC fluorescence staining was visualized in PC-3 cells at 0 h of zinc treatment. The intensity of DAEC fluorescence in the cytosol of PC-3 cells began to increase at the 4-h timepoint, and stronger DAEC fluorescence staining was dispersed throughout the whole cytosol of PC-3 cells following 8 and 12 h of zinc treatment. Additionally, a notable morphological change was observed at 24 h, with the volume of PC-3 cells increasing compared with that of 0-h cells. Similar results were observed in LNCaP cells. The intensity of DAEC fluorescence gradually increased in LNCaP cells with longer zinc treatment time, and stronger DAEC fluorescence was observed in the cytosol of LNCaP cells at both 8 and 12 h of zinc treatment.

Next, the relative amounts of DAEC-sensitive zinc were assessed. In PC-3 cells, the zinc density at 0 h was 0.4 ± 0.15 nmol/ 10^6 cells. The zinc density values significantly increased with extended zinc treatment times, which were 1.8 ± 0.16 nmol/ 10^6 cells at 4 h, 2.4 ± 0.12 nmol/ 10^6 cells at 8 h, 2.3 ± 0.15 nmol/ 10^6 cells at 12 h, and 1.9 ± 0.20 nmol/ 10^6 cells at 24 h. Compared with PC-3 cells with 0 h of zinc treatment, the zinc density values of PC-3 cells incubated with zinc (4, 8, 12, and 24 h) were all statistically significantly different ($P < 0.05$; *Figure 1B*). The results in LNCaP cells were similar to those in PC-3 cells, with the zinc density values estimated to be 0.6 ± 0.13 , 2.6 ± 0.11 , 3.7 ± 0.19 , 3.8 ± 0.07 , and 3.3 ± 0.10 nmol/ 10^6 cells for 0, 4, 8, 12, and 24 h, respectively. The zinc density values at 4, 8, 12, and 24 h of incubation were significantly higher than that at 0 h ($P < 0.05$; *Figure 1B*).

Apoptosis induced by zinc treatment in PC-3 and LNCaP cells

To investigate the effect of zinc on prostate cancer cell apoptosis, Hoechst 33342 staining was performed as an indicator of apoptosis. As shown in *Figure 2A*, the nuclear DNA staining of zinc-treated PC-3 and LNCaP cells with Hoechst 33342 indicated that nuclear fragmentation and chromatin condensation increased with the extension of zinc treatment time. These results suggest that the

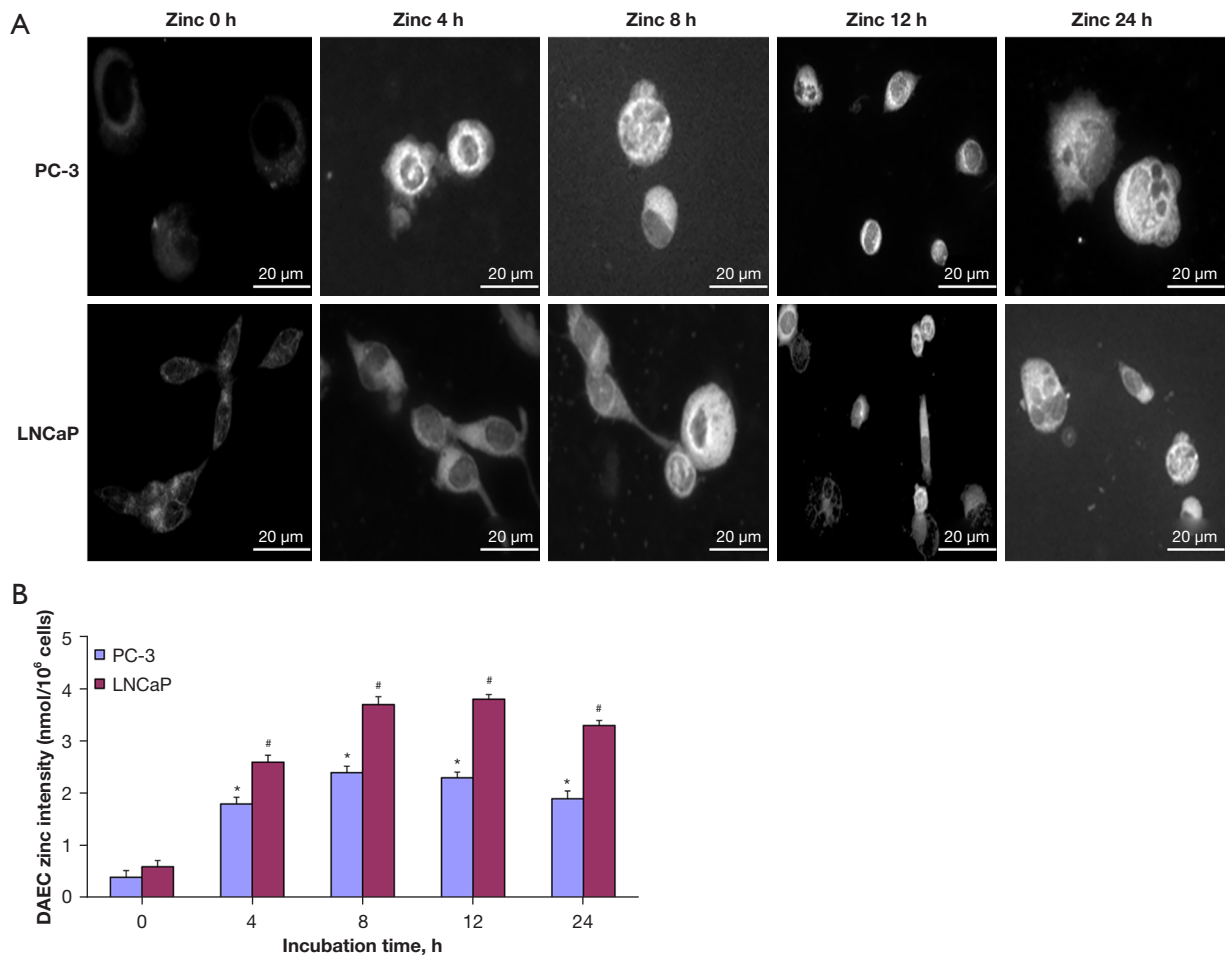


Figure 1 The distribution and density of zinc in PC-3 and LNCaP cells. (A) The zinc distribution at 0, 4, 8, 12, and 24 h was observed under fluorescence microscopy. In both PC-3 and LNCaP cells, DAEC fluorescence staining was observed to be significant at 8 and 12 h, and the volume of PC-3 cells began to increase at 24 h. (B) The zinc density in prostate cancer cells gradually increased with the extension of zinc treatment time. After 8, 12, and 24 h of zinc treatment, the zinc density in prostate cancer cells was significantly higher than that at 0 h. *, compared with 0 h, the results were statistically significant in PC-3 cells ($P < 0.05$); #, compared with 0 h, the results were statistically significant in LNCaP cells ($P < 0.05$). DAEC, dansylaminoethyl-cyclen.

increase in apoptosis levels occurred in a zinc incubation time-dependent manner, with the most accumulation of nuclear fragmentation and chromatin condensation observed in both PC-3 and LNCaP cells at 24 h of zinc treatment. For quantification of apoptotic prostate cancer cells, the nuclear fragmentation levels in PC-3 and LNCaP cells were judged by counting the presence of Hoechst-positive stained fluorescent fragments. The rates of Hoechst-positive nuclear fragmentation with different zinc treatment times in PC-3 cells were $1.2\% \pm 0.01\%$ at 0 h, $5.6\% \pm 1.05\%$ at 4 h, $18.3\% \pm 3.85\%$

at 8 h, $39.4\% \pm 6.21\%$ at 12 h, and $78.3\% \pm 9.16\%$ at 24 h. Compared with the apoptosis rates of PC-3 cells with 0 h of zinc treatment, the apoptosis levels were significantly higher at 8, 12, and 24 h ($P < 0.05$; *Figure 2B*). Additionally, the results in LNCaP cells showed that the rates of Hoechst-positive nuclear fragmentation with different zinc treatment times were $0.8\% \pm 0.01\%$ at 0 h, $4.1\% \pm 1.80\%$ at 4 h, $11.8\% \pm 3.62\%$ at 8 h, $31.7\% \pm 7.92\%$ at 12 h, and $66.8\% \pm 12.14\%$ at 24 h. We also found that the apoptosis levels with 8, 12, and 24 h of zinc treatment were higher than that of LNCaP cells at 0 h ($P < 0.05$; *Figure 2B*).

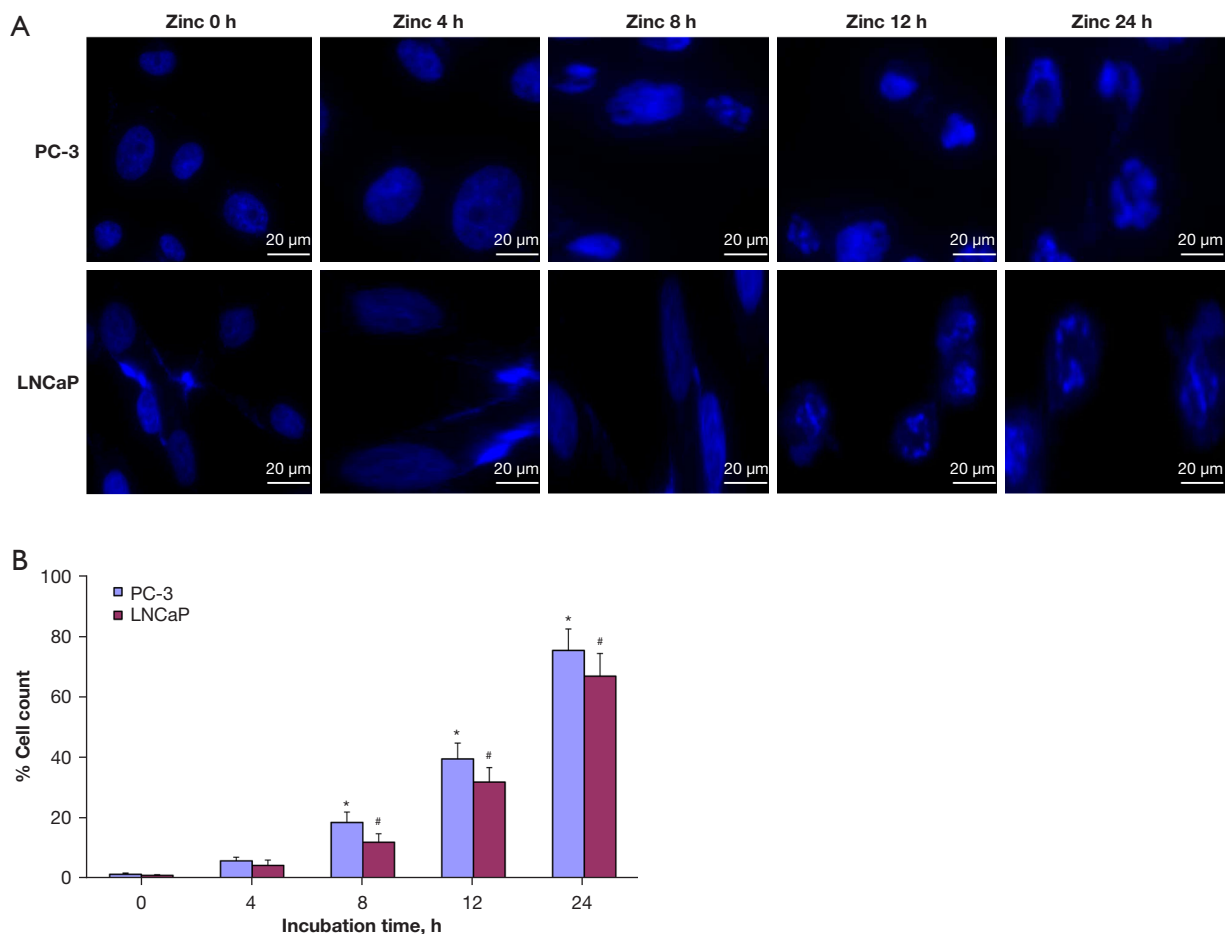


Figure 2 The apoptosis of PC-3 and LNCaP cells was detected by Hoechst 33342. (A) After PC-3 and LNCaP cells were exposed to zinc, Hoechst 33342 staining showed that the levels of nuclear fragmentation and chromatin condensation increased gradually with extended zinc treatment time and were the most significant at 24 h. (B) The positive rates of nuclear fragmentation in PC-3 and LNCaP cells were calculated using Hoechst 33342 staining. The results showed that the rate of nuclear fragmentation in PC-3 and LNCaP cells began to increase significantly after zinc treatment at 8, 12, and 24 h. *, compared with 0 h, the results were statistically significant in PC-3 cells ($P < 0.05$); #, compared with 0 h, the results were statistically significant in LNCaP cells ($P < 0.05$).

Furthermore, prostate cells were double-stained with PI and Annexin-FITC to determine the level of apoptosis induced by zinc. Positive staining with PI indicates necrotic cells, while staining with Annexin-FITC indicates apoptotic cells. In *Figure 3*, the results of flow cytometry are shown, with the lower right quadrant representing apoptotic cells with positive Annexin-FITC staining; there appears to be significant accumulation of cells in the upper right quadrant, indicating a high number of necrotic prostate cancer cells with positive PI staining. The apoptosis levels of PC-3 cells began to increase significantly at 8 h of zinc treatment. After 24 h, PC-3

cell necrosis was observed. Similar results were found in LNCaP cells.

TR3 messenger RNA (mRNA) expression in PC-3 and LNCaP cells treated with zinc

To investigate the TR3 mRNA expression levels following various zinc incubation times both PC-3 and LNCaP prostate cancer cells were treated with zinc as described above and was followed by TR3 mRNA expression analysis with qRT-PCR. The results indicate that there were no significant differences in TR3 mRNA expression levels

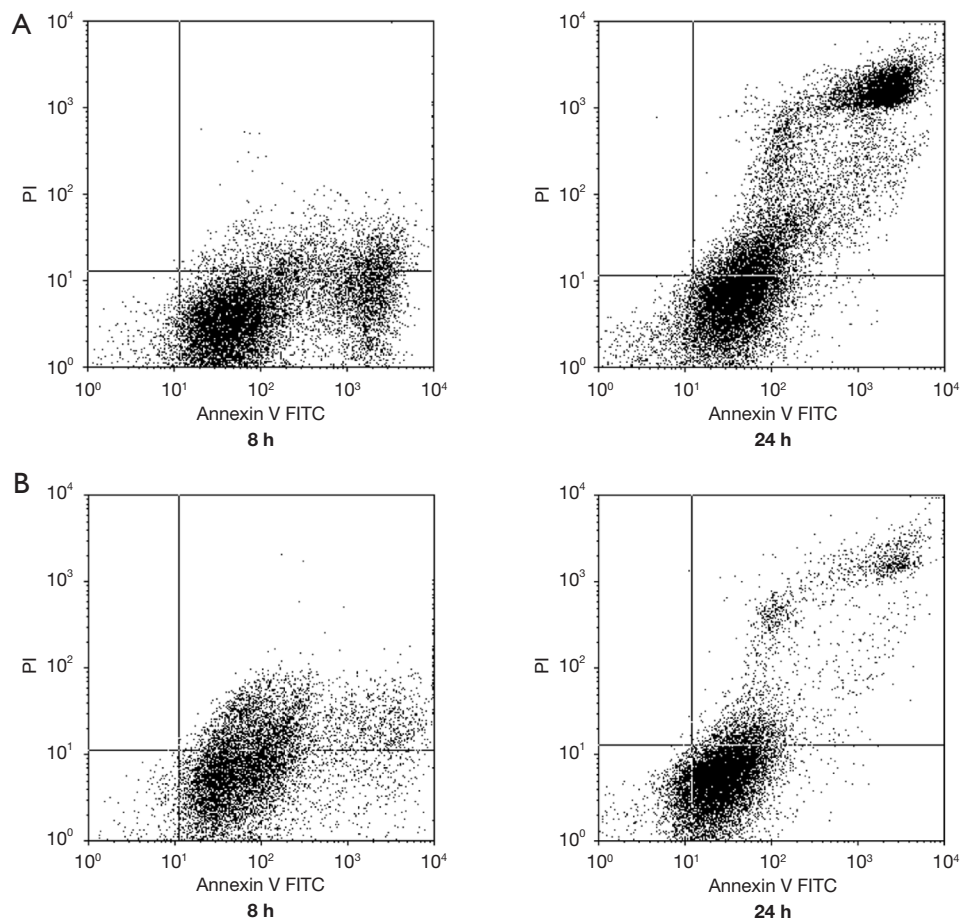


Figure 3 Flow cytometry results of apoptosis levels in PC-3 and LNCaP cells treated with zinc. (A) The apoptosis levels of PC-3 cells began to increase at 8 h of zinc treatment and then increased significantly at 24 h. PC-3 cell necrosis was also observed at 24 h. (B) In LNCaP cells, similar results were observed at 8 and 24 h of zinc treatment. FITC, fluorescein isothiocyanate; PI, propidium iodide.

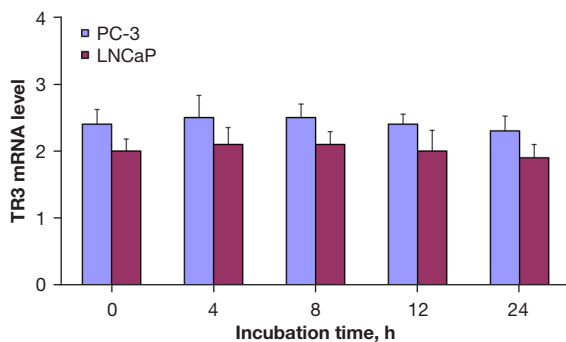


Figure 4 Quantitative real time-polymerase chain reaction was used to detect the TR3 mRNA expression levels in prostate cancer cells treated with zinc. The results show that there was no significant change in the TR3 mRNA expression levels in the PC-3 or LNCaP cells after different zinc treatment times (0, 4, 8, 12, and 24 h; $P > 0.05$). mRNA, messenger RNA.

among the different zinc treatment times in either the PC-3 or LNCaP cells (Figure 4).

Release of cytochrome c from the mitochondria into the cytosol through mitochondrial targeting of TR3 protein was involved in the mechanism of zinc-induced apoptosis in PC-3 and LNCaP cells

To determine the effect of the TR3 protein on the relocation of cytochrome c from the mitochondria to the cytosol, PC-3 and LNCaP cells were treated with zinc for different durations, after which we evaluated the translocation of TR3 protein using green fluorescence FITC staining. Subsequently, the mitochondria were stained with the antibody against mitochondria-specific protein HSP60, which was followed by the application of

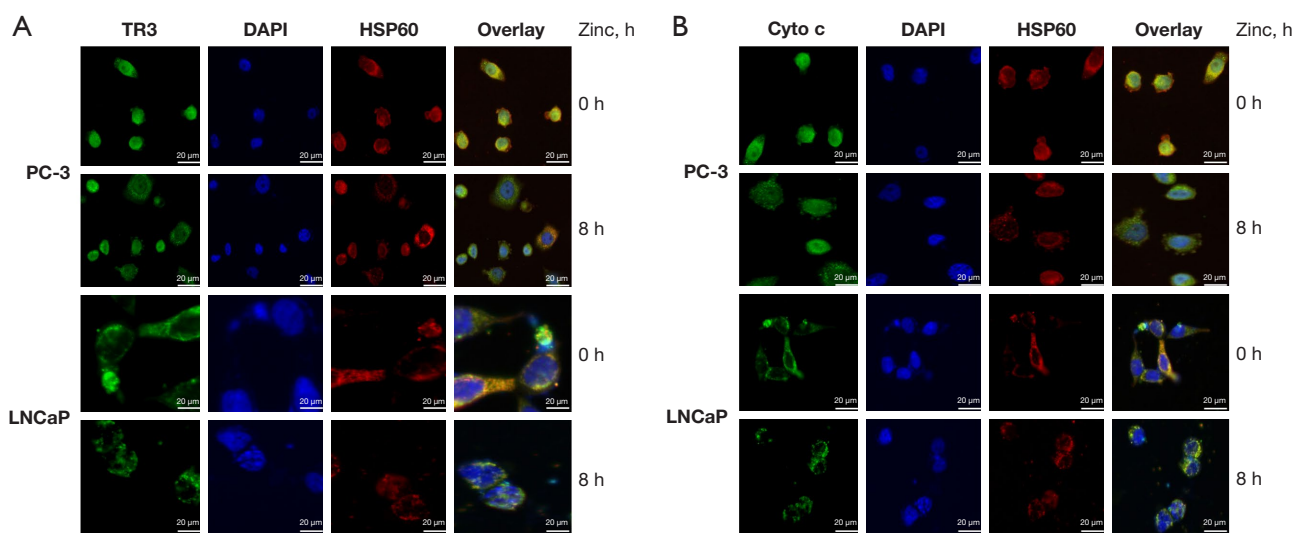


Figure 5 Immunofluorescence costaining results were observed under a confocal microscope. (A) The TR3-FITC protein was localized in the nuclei of PC-3 and LNCaP cells at 0 h and then started to diffusely distribute into the mitochondria at 8 h of zinc treatment. (B) Cytochrome c was present in the mitochondria of PC-3 and LNCaP cells at 0 h of zinc treatment and then dispersed into the cytosol at 8 h. Cyto c, cytochrome c; FITC, fluorescein isothiocyanate; HSP60, heat shock protein 60.

DAPI to the nuclei. Costaining of TR3 (FITC), nuclei (DAPI), and mitochondria (HSP60) was visualized under a confocal microscope. The results showed that in both PC-3 and LNCaP cells, the TR3-FITC protein was localized in the nucleus of prostate cancer cells at 0 h and then started to diffusely distribute into the mitochondria after 8 h of zinc treatment (*Figure 5A*).

In *Figure 5B*, immunofluorescence staining for cytochrome c was performed to detect the relocation of cytochrome c in PC-3 cells following zinc treatment. The mitochondria and nuclei were stained as described above. The translocation pattern showed that cytochrome c was present in the mitochondria of PC-3 and LNCaP cells at 0 h of zinc treatment and then dispersed into the cytosol after 8 h.

Analysis of mitochondrial membrane potential in PC-3 and LNCaP cells following zinc treatment

Loss of mitochondrial membrane potential ($\Delta\psi_m$) was believed to be associated with the release of cytochrome c, which was significantly involved in the mechanism of zinc-induced apoptosis. Analysis of mitochondrial membrane potential collapse with fluorescence microscopy using a MitoLight probe indicated that zinc treatment resulted in a significant loss of mitochondrial membrane potential in both PC-3 and LNCaP cells. *Figure 6* shows the PC-3 and

LNCaP cells at 0 h: the red fluorescence represents healthy cells and the green fluorescence indicates apoptotic cells. The data suggest that the green fluorescence gradually increased in both PC-3 and LNCaP cells with the extension of zinc treatment time, which was accompanied by the disappearance of the red fluorescence.

Discussion

The results of this study suggest that zinc supplementation may play a very important role in inducing apoptosis in both PC-3 and LNCaP prostate cancer cell lines. After PC-3 and LNCaP cells were incubated with exogenous zinc ions (100 μM), zinc density in both cell lines increased with extended incubation time in an apparent time-dependent manner. In PC-3 and LNCaP cells, the cellular zinc density values were significantly higher at 8, 12, and 24 h of treatment compared with that at 0 h. Morphological observation of nuclear fragmentation in both PC-3 and LNCaP cells with Hoechst 33342 staining under fluorescent microscopy showed that zinc could induce apoptosis in prostate cancer cells, with the nuclear fragmentation rate increasing significantly at the 8-, 12-, and 24-h timepoints. Additionally, apoptosis levels were also measured using flow cytometry analysis of Annexin-FITC and PI-stained PC-3 and LNCaP cells, which also suggested that apoptosis rates

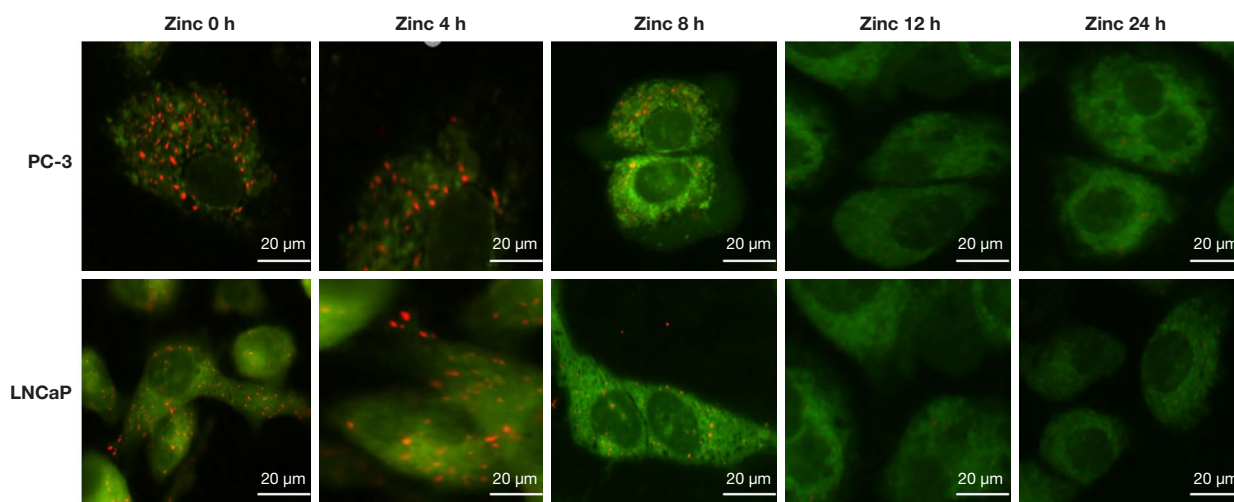


Figure 6 The changes in mitochondrial membrane potential in PC-3 and LNCaP cells were detected using a MitoLight probe. Red fluorescence represents the stable state of PC-3 and LNCaP cells, while green fluorescence indicates apoptotic cells. With the extension of zinc treatment time, the red fluorescence gradually disappeared in PC-3 and LNCaP cells, while the green fluorescence increased. This indicates that the mitochondrial membrane potential gradually disappeared with increasing apoptosis.

increased 8 h after zinc treatment. Necrosis was observed at 24 h. Furthermore, with zinc treatment, TR3 protein translocation was noted from the nucleus to the mitochondria and accompanied by cytochrome c release to the cytosol. However, no significant changes in TR3 mRNA expression levels were observed.

The loss of zinc in prostate cancer cells is an important change that occurs with prostate cancer development and progression, and zinc concentrations have been demonstrated to be reduced by 60–70% in blood serum and prostate cancer tissues (10). Therefore, reestablishing high zinc levels in prostate cancer cells may be a useful strategy to inducing apoptosis and possibly controlling malignant proliferation. A previous study also indicated that zinc could induce apoptosis in PC-3 cells by enhancing their chemosensitivity to paclitaxel. The mechanism was mainly through decreasing the Bcl-2 to Bax ratio, with increased expression of cleaved caspase 3 and cleaved caspase 9 (11). As a downstream protein of zinc, hexokinase 2 expression was disrupted by zinc treatment and could induce apoptosis of prostate cancer cells. This was mediated by protein kinase B (Akt) inhibition and glycogen synthase kinase 3 β (GSK3 β) activation (12). Our data show that intracellular zinc can induce apoptosis in both PC-3 and LNCaP cells, with a significant time–response relationship between apoptosis levels and zinc incubation time.

As an orphan receptor, TR3 is a member of the steroid-

thyroid hormone-retinoid receptor superfamily of transcription factors. TR3 protein overexpression has also been reported in certain types of cancers and as a target of anticancer treatment through inducing cancer cell apoptosis and suppressing tumor metastasis (13,14). The TR3-Bcl-2 protein complex in mitochondria could influence apoptosis by acting on several molecular regulators involved in programmed cell death and also inhibit the growth of malignant cells (15). Previous results indicated that TR3 is involved in inducing apoptosis through upregulating E2F1 in LNCaP cells (16). Furthermore, the expression of TR3 has been reported in prostate cancer, previous study revealed that TR3 expression level was positively correlated with that of androgen receptor (AR), which mediated by increasing the production of AR splice variants (17). In this study, TR3 was demonstrated to be an important target in zinc-induced apoptosis of both PC-3 and LNCaP cells. These effects were mediated by the translocation of TR3 from the nucleus to mitochondria, without any significant change in TR3 mRNA expression levels after zinc incubation.

Cytochrome c is associated with the inner membrane of the mitochondria and serves as an essential component of the electron transport chain. It is involved in redox reactions and is released from the mitochondria following stimulation and induction of apoptosis (18). The effect of apoptosis mediated through cytochrome c has been

associated with changes in the mitochondrial membrane potential. Feng *et al.* reported that exogenous zinc could increase Bax expression in the mitochondrial outer membrane and subsequently release cytochrome c into the cytosol, inducing apoptosis in PC-3 cells (19). In this study, we observed through immunofluorescence experiments that cytochrome c release and apoptosis induced by mitochondrial targeting of TR3 were involved in inhibiting the malignant proliferation of PC-3 and LNCaP human prostate cancer cells. Additionally, a loss of mitochondrial membrane potential in these cells was the main factor leading to cytochrome c release into the cytosol. Furthermore, the consistent and persistent effect of zinc on apoptosis rates in PC-3 and LNCaP cells occurred in a time-dependent manner, with apoptosis levels increasing with extended zinc treatment times.

Conclusions

Overall, our data demonstrate that exposure to zinc could increasingly induce apoptosis in both PC-3 and LNCaP cells over a 24-h treatment period, and this effect appeared to be time-dependent. Following zinc exposure, TR3 protein translocated from the nucleus to the mitochondria and was accompanied by cytochrome c release into the cytosol from the mitochondria. However, no significant changes in TR3 mRNA expression levels were observed. Overall, our findings indicate that zinc can play an inhibitory role in prostate cancer by inducing apoptosis, which dependent on mitochondrial apoptosis pathway. Nevertheless, zinc as a drug for prostate cancer still needs a lot of research.

Acknowledgments

Funding: None.

Footnote

Reporting Checklist: The authors have completed the MDAR reporting checklist Available at <https://tau.amegroups.com/article/view/10.21037/tau-23-61/rc>

Data Sharing Statement: Available at <https://tau.amegroups.com/article/view/10.21037/tau-23-61/dss>

Peer Review File: Available at <https://tau.amegroups.com/article/view/10.21037/tau-23-61/prf>

Conflicts of Interest: All authors have completed the ICMJE uniform disclosure form (available at <https://tau.amegroups.com/article/view/10.21037/tau-23-61/coif>). The authors have no conflicts of interest to declare.

Ethical Statement: The authors are accountable for all aspects of the work in ensuring that questions related to the accuracy or integrity of any part of the work are appropriately investigated and resolved.

Open Access Statement: This is an Open Access article distributed in accordance with the Creative Commons Attribution-NonCommercial-NoDerivs 4.0 International License (CC BY-NC-ND 4.0), which permits the non-commercial replication and distribution of the article with the strict proviso that no changes or edits are made and the original work is properly cited (including links to both the formal publication through the relevant DOI and the license). See: <https://creativecommons.org/licenses/by-nc-nd/4.0/>.

References

1. Siegel RL, Miller KD, Jemal A. Cancer statistics, 2020. *CA Cancer J Clin* 2020;70:7-30.
2. Preisser F, Wang N, Abrams-Pompe RS, et al. Oncologic outcomes of organ-confined Gleason grade group 4-5 prostate cancer after radical prostatectomy. *Urol Oncol* 2022;40:161.e9-161.e14.
3. Wang C, Zhang Y, Gao WQ. The evolving role of immune cells in prostate cancer. *Cancer Lett* 2022;525:9-21.
4. Miyahira AK, Zarif JC, Coombs CC, et al. Prostate cancer research in the 21st century; report from the 2021 Coffey-Holden prostate cancer academy meeting. *Prostate* 2022;82:169-81.
5. Vigneswaran HT, Jagai JS, Greenwald DT, et al. Association between environmental quality and prostate cancer stage at diagnosis. *Prostate Cancer Prostatic Dis* 2021;24:1129-36.
6. Singh CK, Chhabra G, Patel A, et al. Dietary Phytochemicals in Zinc Homeostasis: A Strategy for Prostate Cancer Management. *Nutrients* 2021;13:1867.
7. Wang J, Zhao H, Xu Z, et al. Zinc dysregulation in cancers and its potential as a therapeutic target. *Cancer Biol Med* 2020;17:612-25.
8. Song X, Yuan B, Zhao S, et al. Effect of taurine on the proliferation, apoptosis and MST1/Hippo signaling in prostate cancer cells. *Transl Cancer Res* 2022;11:1705-12.

9. Hong SH, Choi YS, Cho HJ, et al. Antiproliferative effects of zinc-citrate compound on hormone refractory prostate cancer. *Chin J Cancer Res* 2012;24:124-9.
10. Zhao Y, Tan Y, Dai J, et al. Zinc deficiency exacerbates diabetic down-regulation of Akt expression and function in the testis: essential roles of PTEN, PTP1B and TRB3. *J Nutr Biochem* 2012;23:1018-26.
11. Zhang P, Li Y, Tang X, et al. Zinc enhances chemosensitivity to paclitaxel in PC-3 prostate cancer cells. *Oncol Rep* 2018;40:2269-77.
12. Xue YN, Yu BB, Li JL, et al. Zinc and p53 disrupt mitochondrial binding of HK2 by phosphorylating VDAC1. *Exp Cell Res* 2019;374:249-58.
13. Zhan YY, He JP, Chen HZ, et al. Orphan receptor TR3 is essential for the maintenance of stem-like properties in gastric cancer cells. *Cancer Lett* 2013;329:37-44.
14. Chen HZ, Liu QF, Li L, et al. The orphan receptor TR3 suppresses intestinal tumorigenesis in mice by downregulating Wnt signalling. *Gut* 2012;61:714-24.
15. Chen X, Cao X, Tu X, et al. BI1071, a Novel Nur77 Modulator, Induces Apoptosis of Cancer Cells by Activating the Nur77-Bcl-2 Apoptotic Pathway. *Mol Cancer Ther* 2019;18:886-99.
16. Mu X, Chang C. TR3 orphan nuclear receptor mediates apoptosis through up-regulating E2F1 in human prostate cancer LNCaP cells. *J Biol Chem* 2003;278:42840-5.
17. Tran TT, Lee K. TR3 Enhances AR Variant Production and Transactivation, Promoting Androgen Independence of Prostate Cancer Cells. *Cancers (Basel)* 2022;14:1911.
18. Hüttemann M, Pecina P, Rainbolt M, et al. The multiple functions of cytochrome c and their regulation in life and death decisions of the mammalian cell: From respiration to apoptosis. *Mitochondrion* 2011;11:369-81.
19. Feng P, Li T, Guan Z, et al. The involvement of Bax in zinc-induced mitochondrial apoptosis in malignant prostate cells. *Mol Cancer* 2008;7:25.

(English Language Editor: J. Gray)

Cite this article as: Ma D, Guo Y, Fu Y, Wu J, Ren R. Temporal relationship of the orphan receptor TR3 translocation and expression with zinc-induced apoptosis in prostate cancer cells. *Transl Androl Urol* 2023;12(3):444-454. doi: 10.21037/tau-23-61